Redundant Single Gimbal Control Moment Gyroscope Singularity Analysis

Nazareth S. Bedrossian,* Joseph Paradiso,† and Edward V. Bergmann‡
Charles Stark Draper Laboratory, Inc., Cambridge, Massachusetts 02139
and
Derek Rowell§
Massachusetts Institute of Technology, Cambridge, Massachusetts 02139

The robotic manipulator is proposed as the mechanical analog to single gimbal control moment gyroscope systems, and it is shown that both systems share similar difficulties with singular configurations. This analogy is used to group gimbal angles corresponding to any momentum state into different families. The singularity problem associated with these systems is examined in detail. In particular, a method is presented to test for the possibility of nontorque-producing gimbal motion at a singular configuration, as well as to determine the admissible motions in the case when this is possible. Sufficient conditions are derived for instances where the singular system can be reconfigured into a nonsingular state by these nontorque-producing motions.

I. Introduction

SINGLE gimbal control moment gyroscopes (SGCMGs) are angular momentum storage devices that can be used as torque actuators for spacecraft attitude control. Since they operate exclusively on electric power, CMGs can provide torque without expending fuel or consumables. Single-gimbal CMGs have significant hardware advantages over double-gimbal CMGs in spacecraft attitude control; i.e., mechanical simplicity and ability to provide torque amplification. Despite these advantages, SGCMGs are plagued by copious mathematical singular states that preclude torque generation in a certain direction. This situation occurs when all individual CMG torque outputs are perpendicular to the singular direction, or equivalently when the individual momenta have extremal projections onto this direction. These conditions, if not properly addressed, severely limit the usable momentum capability of the CMG system. Hardware limits on gimbal rates entail that neighborhoods of singular states also be considered in the control law design since they represent regions of limited torque capability. Although the extra degrees of freedom provided by adopting redundant CMG systems may reduce the possibility of encountering singular states, their use does not eliminate the singularity problem. Since the specific arrangement of the gimbals affects the type and number of singularities, one may reduce the possibility of encountering singular states within the CMG momentum volume through modification and improvements in CMG design.[1-3]

The groundwork for the singularity analysis of SGCMG systems was presented in Ref. 4, where the topology of such devices was explored in a systematic fashion. One of the contributions of this paper was the establishment of a mathematical framework to characterize and describe the geometric properties of singular states. In particular, an approach to analyze nontorque-producing motions (or null motion) near singular configurations was presented. A refinement of this method was given in Ref. 5.

Received March 10, 1989; revision received July 31, 1989.

*Graduate Student, Department of Mechanical Engineering, Massachusetts Institute of Technology.

†Member of Technical Staff.

‡Section Chief, Flight Systems.

§Associate Professor, Department of Mechanical Engineering.

In this paper the robotic manipulator is shown to be the mechanical analog to SGCMGs and is used as an aid to the analysis of SGCMG systems. Both systems possess similar difficulties with singular configurations, and results from one area may be applicable to the other. As a result of this correspondence, the analog is used to group CMG gimbal angle configurations into different families for any momentum state. The singularity problem associated with SGCMGs is then examined in detail, and a method is presented to test for the possibility of nontorque-producing gimbal motion at a singular configuration. In this way, it is possible to distinguish between different types of singularities. In the case where null motion is possible at a singular configuration, this approach allows for the determination of these admissible motions, and sufficient conditions are derived for the case when the singular system can be reconfigured into a nonsingular state. Several examples assuming a four-SGCMG, pyramid-mounted system are presented to illustrate these concepts.

II. Mechanical Analog

In this section, the robotic manipulator is proposed as the mechanical analog to SGCMGs. The correspondence between robotic manipulators and SGCMGs can be exploited to aid in the understanding and design of steering laws. To establish the correspondence, we will establish the analogy between momentum and position, torque and velocity, and demonstrate the equivalence of the singularity problem for both devices.

One approach in the analysis of CMG and manipulator systems is to consider their action as a mapping from an input to an output space. For a system of n SGCMGs, denote the space of gimbal angles θ_i by T^n (the n-dimensional torus since $\theta_i = \theta_i + 2\pi$) and momentum space by $H \subset \boldsymbol{R}^3$. Similarly, for an n-link, serial, open-loop manipulator, denote the space of joint coordinates q_i by T^n and position space by $X \subset \boldsymbol{R}^3$. In this paper the manipulator end-effector orientation is not considered. Each q_i can be either a rotational or translational joint. The displacement of each link is expressed by $\boldsymbol{x}_i$, which is the projection of the ith link in the base (absolute) frame of reference, with positive direction defined by proceeding outward along the kinematic chain. For both systems, we can define the nonlinear, differentiable, vector-valued mappings, f: $T^n \rightarrow H$ and g: $T^n \rightarrow X$, the former for CMGs and the latter for manipulators.

To establish the correspondence between momentum and position, consider the CMG system as an open-loop kinematic chain or linkage made up of equal "length" momentum links

$h_i(\theta_i)$ attached to each other in arbitrary order. The length of each link is given by the magnitude of each CMG angular momentum. The individual momentum vectors are constrained to rotate in a fixed plane determined by the corresponding gimbal axis. This requirement is not necessary for general spatial manipulators. The motivation for this concept derives from the expression for the total angular momentum $h(t)$ of an SGCMG system as the vector sum of individual momenta, i.e.,

$$h(t) = \sum_{i=1}^{n} h_i\left[\theta_i(t)\right] = f\left[\theta(t)\right]$$

For a robotic manipulator, the end-effector position $x(t)$ is the vector sum of individual link displacements $x_i(q)$.

$$x(t) = \sum_{i=1}^{n} x_i\left[q(t)\right] = g\left[q(t)\right]$$

The summation operation in both cases is commutative.

In similar fashion, the analogy between torque and velocity can be established. The total output torque for an SGCMG system is given by the time rate of change of the total system angular momentum relative to a frame of reference, in this case the spacecraft body-fixed coordinate frame, which is given by

$$\dot{h}(t) = \sum_{i=1}^{n} \dot{h}_i\left[\theta_i(t)\right] = J\left[\theta(t)\right]\dot{\theta}(t)$$

Similarly, for the robotic manipulator, the end-effector velocity is

$$\dot{x}(t) = \sum_{i=1}^{n} \dot{x}_i\left[q(t)\right] = J\left[q(t)\right]\dot{q}(t)$$

where, in both cases, $J = [j_1, \ldots, j_n]$ is the $3 \times n$ Jacobian transformation matrix. Obviously, commutativity applies here as well. To complete the analogy, the following discussion illustrates the equivalence in the singularity problem for manipulator and the SGCMG systems.

The singularity problem involves the same concept for both devices. In both cases, singularity is defined when the mapping from input to output space is not locally onto, or equivalently the Jacobian matrix does not have full rank, i.e., rank $(J) < 3$. For the the CMG case, torque cannot be generated along a particular axis, whereas for manipulators, end-effector motion is impossible in the singular direction. The correspondence between manipulators and SGCMG systems is summarized in Fig. 1.

III. Classification of Families of Gimbal Angle Solutions

In this section a method will be presented to classify families of gimbal angle solutions for SGCMG systems. This notion of families of solutions can be a useful tool in the process of designing CMG steering laws. This method is motivated by the use of the mechanical analog to identify CMG gimbal angle configurations belonging to the same family as the total momentum of the CMG system varies. The notion of "family of solution" is well established for manipulators. The fundamental concept in defining a family is the use of the minors of the Jacobian matrix. For nonredundant manipulators, only two configurations exist for a given end effector location, and the boundary of the two solutions is defined by $\det(J) = 0$. In this case, the Jacobian is square $(m \times m)$, and has only one minor of order m. The two configurations are defined by the sign of the Jacobian determinant (+ and −). For redundant manipulators, the Jacobian is nonsquare $(m \times n, n > m)$, and multiple solutions may exist for a given end-effector location.These solutions are similarly identified by the nonzero minors of the Jacobian.[6,7] For further detail see Ref. 8.

MANIPULATOR		⇔	SG CMG SYSTEM	
Position	$\underline{x} = \underline{x}(\underline{q})$		Momentum	$\underline{h} = \underline{h}(\underline{\theta})$
Velocity	$\dot{\underline{x}} = J(\underline{q})\,\dot{\underline{q}}$		Torque	$\dot{\underline{h}} = J(\underline{\theta})\,\dot{\underline{\theta}}$
Acceleration	$\ddot{\underline{x}} = J(\underline{q})\,\ddot{\underline{q}} + \dot{J}(\underline{q})\,\dot{\underline{q}}$		Torque	$\ddot{\underline{h}} = J(\underline{\theta})\,\ddot{\underline{\theta}} + \dot{J}(\underline{\theta})\,\dot{\underline{\theta}}$
		Singularity		
No motion possible in a certain direction			No torque possible in a certain direction	

Fig. 1 Correspondence of manipulators to SGCMG systems.

In the case of SGCMGs, we can apply this notion of nonzero minors as a method of classifying multiple gimbal angle solutions for a given momentum state. It will be assumed that no restrictions are placed on gimbal angle rotations, as is the usual situation.

Definition: An admissible family of gimbal angle solutions is the set

$$A = \left\{\theta \in D:\ \ M_i(\theta) \neq 0,\ \ \forall i \leq n\,(n-1)\,(n-2)/3!,\ \ n \geq 3\right\}$$

where M_i are distinct Jacobian minors of order 3, and $D = \left\{\theta \in T^n\!: h = f(\theta)\right\}$ is the admissible domain for a given total momentum state.

With this definition, the various gimbal angle solutions for all momentum states may be classified by the sign combinations of the Jacobian minors. As a result, switching between different families is accomplished any time a minor changes sign. Note that it is not necessary that all minors be zero (i.e., singular state) for switching to occur. The boundaries of the families (either in gimbal or momentum space) are generated by the gimbal angle solutions to singular minors i.e., all θ such that $M_i(\theta) = 0$. The singular states correspond to the intersections in gimbal space of all of these singular minors. It is also evident that a table of all possible sign combinations can be generated for the minors similar to the sign pattern of CMG rotor momentum projections onto the singular direction.[4,9] It should be emphasized, however, that not all sign combinations are admissible for a given momentum state, since the solution gimbal angles may violate the total momentum constraint. This means that only a subset of all possible minors can be considered at any momentum state.

To illustrate this concept, switching between solution families is examined for a four-pyramid CMG system. It will be shown that different families are connected via null motion [that is, $\delta\theta$ such that $J(\theta)\delta\theta = 0$], and switching can occur at nonsingular states. The momentum state was chosen as $h = [0.5, 0.0, 0.0]^T$ corresponding to the gimbal angle configuration $\theta = [-18, 0.4, 43.8, -22.9]^T$ (in degrees). The gimbal rates for null motion of unit magnitude in the direction of the Jacobian null vector were determined according to

$$\dot{\theta} = \frac{1}{\|n\|_2} n$$

where

$$n = \frac{\partial h_1}{\partial \theta} \wedge \frac{\partial h_2}{\partial \theta} \wedge \frac{\partial h_3}{\partial \theta} = \left[C_1, C_2, C_3, C_4\right], \text{ Jacobian null vector}$$

$C_i = (-1)^{i+1} M_i$, order 3 Jacobian cofactor

$M_i = \det(J_i)$, order 3 Jacobian minor

$J_i = J$, with ith column removed

Here, n represents the one-dimensional Jacobian null-space basis vector. This vector is generated using the generalized cross or wedge product[10] $\wedge$ to form the vector orthogonal to the three Jacobian row vectors.[8] The integration time step was 0.01 s. In the case when more than four CMGs are used, the minors can be formed from all distinct permutations of three columns of the Jacobian matrix. That is, each minor corresponds to the determinant of each distinct 3×3 submatrix that can be formed from the Jacobian matrix. From Fig. 2, it is seen that the singularity measure, $\sqrt{\det(JJ^T)}$ remains nonzero, and thus the system is nonsingular for the entire simulation period. The reason for using the square root of the determinant is that this expression is equal to the product of the singular values of the Jacobian matrix, and the system is singular when one of these singular values is zero.[8] From the minor plots, transitions between seven distinct families (Table 1) can be observed. The switching sequence is given by {2, 3, 4, 5, 4, 6, 7, 1, 2}. From the gimbal angle plots, the closed periodic nature of the null gimbal angle trajentory is evident. Figure 2 indicates that the system remains nonsingular while families were switched during continuous null motion.

Expanding the combinatoric possibilities, it is seen that up to 16 (2^4) possible minor sign combinations can exist. The constraint on total CMG momentum, however, will prevent some from being realized. The periodic nature of switching seen in the preceding example seems to imply that null motion connects these particular families at the assigned value of total momentum; any other possible families may not be reachable from the initial gimbal angle configuration at this momentum level. Analogous tests performed at zero momentum resulted in switching at singular configurations. This seems to imply that boundaries between gimbal angle families are dependent on the total CMG stored momentum, initial gimbal angle orientation corresponding to this momentum level, and perhaps the adopted CMG configuration. Results obtained in Ref. 11 seem to indicate that the initial gimbal configuration must lie in certain regions in order to pass through an arbitrary sequence of momentum states without encountering a singular configuration.

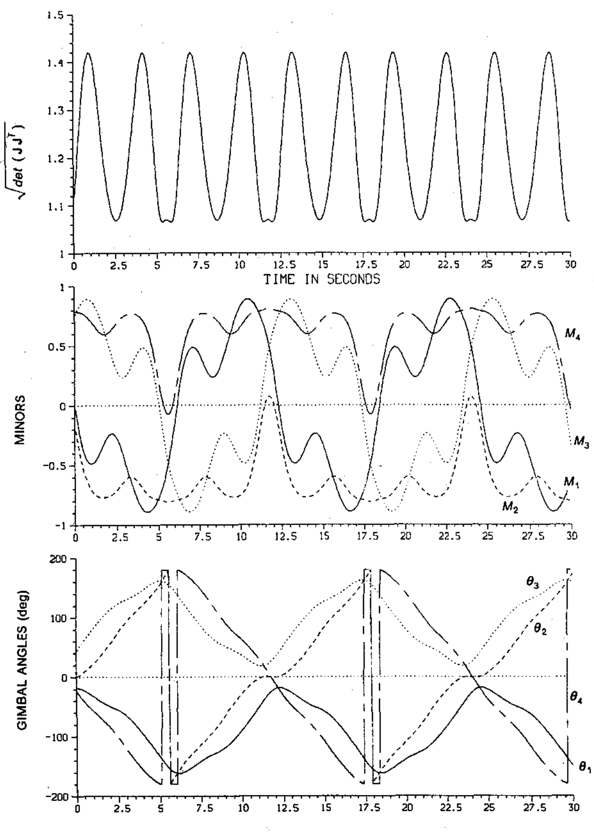

Fig. 2 Switching of families of solutions.

Table 1 Minor sign pattern for families of gimbal angle solutions

Family	M_1	M_2	M_3	M_4
1	+	+	+	+
2	+	−	+	+
3	−	−	+	+
4	−	−	−	+
5	−	−	−	−
6	+	−	−	+
7	+	−	+	+

IV. Singularity Analysis

Before proceeding with the singularity analysis of SGCMG systems, we will briefly review the definition of singularity. The requirement of a control torque in each of the three spacecraft axes is expressed by the rank of the CMG system Jacobian matrix. If rank$(J)<3$, the CMG system is unable to produce torque along an arbitrary direction s, the singular direction. This requirement is summarized in the following definition.

Singular state: A singular state is defined as a set Θ^s of gimbal angles for which

$$\Theta^s = \{\theta^s \in T^n: \langle s, j_i(\theta_i^s)\rangle = 0 \quad \forall i = 1, \ldots, n\} \tag{1}$$

This occurs whenever rank $(J)<3$, where $j_i(\theta_i^s)$ is the ith column of the Jacobian matrix evaluated at the singular gimbal angle. A physical interpretation of the singular direction s can be obtained from the mechanical analog by considering the fundamental relationship between end-effector force and input displacement via the principal of virtual work,[12] which is given by

$$T_a = J^T(q)F_i$$

where T_a represents actuator torque, and F_i represents end-effector (interface) force. Equation (1) can also be written as $J^T s = 0$, from which it can be seen that s plays the role of a workless external force.

Singular states can be classified according to the location of the total momentum vector relative to the momentum volume or work space: 1) surface or saturation singularities or 2) internal singularities (elliptic or unescapable, and hyperbolic).

V. Saturation Singularity

As the name suggests, a saturation singularity corresponds to a configuration for which the CMG system has projected its maximum momentum capability along a certain direction. The mechanical analog to this type of singularity is a completely stretched manipulator. The criteria for a saturation singularity can be summarized as

$$\mathrm{Rank}(J)<3$$

$$s^T \cdot h_i > 0 \qquad \forall i = 1, \ldots, n$$

From the mechanical analog, it is intuitively clear that there can be no relative motion of the links that does not affect the end-effector location. The same comments apply to the CMG system, and no escape is possible.

VI. Internal Singularity

Any singular state for which the total angular momentum vector is inside the momentum envelope (boundary) is defined by default as "internal." These singularities can be further classified according to whether escape by null motion is possible. The term "escape" used in this context is defined as follows.

Escape by null motion: A singular CMG system can be reconfigured by null motion into a nonsingular configuration if one exists. The implications of this statement are twofold.

1) A nonsingular configuration is reachable by null motion from the singular configuration; i.e., the CMG system can be reconfigured in a continuous manner using null motion only. To state it succinctly, the two solution sets are not disjoint with respect to null motion.

2) The rank of the Jacobian can be affected (increased) by these null motions.

With these two criteria in mind, a test for the possibility of escape by null motion is derived in the following section. With slight modifications, this same approach can also be used for the singularity analysis of robotic manipulators.[13]

Before proceeding to the next section, it is important to distinguish between escape by *reconfiguration* and escape by *reorientation* using null motion only. By the latter we mean reorientation of the range space of the singular Jacobian matrix $\mathcal{R}(J^s)$ such that it spans the desired torque direction, since solution gimbal rates can always be computed for torque requests that lie in $\mathcal{R}(J^s)$. Equivalently, the singular direction s is reoriented by null motion [since $s \perp \mathcal{R}(J^s)$] so that it is orthogonal to the desired torque direction. This serves to illustrate the point that for singularity avoidance control algorithms, the singular direction, and not merely the fact that the system is singular, represents the primary constraint on system performance. As long as the desired torque direction lies in $\mathcal{R}(J)$, bounded gimbal rate solutions can always be calculated whether or not J is singular.

A. Test for Possibility of Escape by Null Motion

The test for escape can naturally be separated into two parts. First, we test whether null motion is possible at the given singular state. Obviously, if null motion is impossible, there can be no escape from singularity. Second, if null motion is possible, it is desirable to know whether this motion affects the rank of the Jacobian. For the first part of the test, an approach based on techniques presented in Ref. 4 is adopted.

To test whether null motion is possible at a singularity, the total CMG angular momentum is expanded in a Taylor series about a singular configuration θ^s to obtain

$$h(\theta^s+\delta\theta)-h(\theta^s)=\sum_{i=1}^{n}\left[j_i(\theta_i^s)\delta\theta_i-{}^1\!/_2\, h_i(\theta_i^s)\delta\theta_i^2\right]+\cdots \tag{2}$$

If we now impose the constraint of Eq. (1) by taking the inner product of Eq. (2) with the singular direction s, all of the odd terms on the right-hand side drop out since $s^T \cdot j_i(\theta_i^s)=0$, $i=1,\ldots,n$. The resulting expression becomes

$$s^T\cdot[h-h^s]=s^T\cdot\sum_{i=1}^{n}h_i^s\left[\cos(\delta\theta_i)-1\right] \tag{3}$$

To examine the behavior of Eq. (3) for null variations near a singularity, $h \equiv h^s$ by definition of null motion, and Eq. (3) becomes

$$0=\sum_{i=1}^{n}s^T\cdot h_i^s\left[\cos(\delta\theta_i)-1\right] \tag{4}$$

This is the governing nonlinear constraint equation for infinitesimal null motion about a singular state that must be solved for the admissible null variations consistent with the constraint of Eq. (1). In geometric terms, the purpose of this part of the test is to characterize the nature of the singular state in the configuration (gimbal angle) space Θ, i.e., whether it is an isolated point, a point on a closed curve, at the intersection of multiple curves, ect.

To obtain a solution for $\delta\theta_i$, this equation can be linearized. Expressing the null variations as a linear combination of the Jacobian null space basis vectors as in Ref. 5:

$$\delta\theta=\sum_{i=1}^{n-r(J)}c_i n_i = Nc \tag{5}$$

where

c_i = scalar weighting coefficient
n_i = null space basis vectors
$r(J)$ = rank of Jacobian matrix

Substituting Eq. (5) into Eq. (4), the desired final result is obtained:

$$c^T Q c = 0 \tag{6}$$

where

$Q = N^T P N$
$P = \mathrm{diag}(s^T \cdot h_i^s)$, projection matrix

This quadratic form represents a constraint equation that the admissible null motions must satisfy in the vicinity of a singular state. To find these variations, this equation is solved for c, and the result is substituted in Eq. (5) to form the admissible null variations $\delta\theta_a = Nc_s$, where c_s is the solution to Eq. (6). The solutions to Eq. (6) can be classified according to the properties of the quadratic form as 1) definite Q or 2) indefinite or singular Q.

When condition 1 holds (i.e., $Q>0$), the only solution to Eq. (6) is $c=0$, and null motion is impossible; thus escape is impossible from this type of singular configuration. It is seen that this condition also satisfies Eq. (4) exactly. Note that a sufficient but not necessary condition for $Q>0$ is that $P>0$, an example of which is a saturation singularity. There exist internal singularities, however, for which $Q>0$ while P is not. This type of singularity is termed elliptic, from Ref. 4, and is an isolated point in Θ. In general, this is the most difficult singularity to avoid with steering (redundancy resolution) algorithms and represents the most problematic CMG orientation.

The other possibility for Q is to be indefinite or singular. This type of singularity is termed hyperbolic, from Ref. 4. Although this implies that null motion can be generated at this singularity, the mere possibility of null motion does not guarantee escape from singularity. Degenerate solutions that do not affect the rank of the Jacobian must be excluded. These degenerate solutions are referred to as rigid-body motions because the singular configuration remains undisturbed during the null displacements. In this case, the singular state is a point on null trajectories on Θ, and the admissible null variations are tangent to these trajectories at the singular configuration.

To address the issue of degenerate solutions (i.e., null displacements that generate rigid-body motion and do not change the rank of the Jacobian, as described previously), an additional test must be performed. By examining the Taylor series expansion of the singularity measure $m=\det(JJ^T)$ for admissible null motions obtained from Eq. (4), it can be ascertained whether m can be changed by these null displacements. To characterize the nature of its stationary points, it is natural to consider constrained variations of the singularity measure along null trajectories in Θ. These trajectories are defined as a set of connected points θ, which satisfy $h(\theta^s)=f(\theta)$ and for which $J(\theta)$ has constant rank. From this definition, these trajectories define a manifold.

Geometrically, since it has already been established that the singular state is not an isolated point in configuration space, it must lie either on a manifold or at the intersection of multiple manifolds (including the case of tangent intersections). As an example, a degenerate solution would be one where the singular state lies on a closed curve along which the Jacobian has constant but less than full rank. In this case, the singular state would be a point on a "singular" curve and would represent an unescapable singularity. The opposite situation would occur if the singular state was at the intersection of two curves along which the Jacobian had full rank. In this case, the admissible null motions from Eq. (4) would represent the tangents to these two curves at the point of intersection. Motion along one of these tangents would result in a change in the rank of the Jacobian, and this would represent an escapable singularity.

Expanding m about the singular configuration we obtain

$$m(\boldsymbol{\theta}^s + \delta\boldsymbol{\theta}) = m(\boldsymbol{\theta}^s) + \sum_{i=1}^{n} \frac{\partial m}{\partial \theta_i}\bigg|_{\theta^s} \delta\theta_i + \frac{1}{2}\sum_{j=1}^{n}\sum_{i=1}^{n} \frac{\partial^2 m}{\partial\theta_j \partial\theta_i}\bigg|_{\theta^s} \delta\theta_j\,\delta\theta_i + \cdots \tag{7}$$

The first term on the right-hand side vanishes since $m(\boldsymbol{\theta}^s)=0$ by definition of a singular configuration.[8] The second term also vanishes because $\boldsymbol{\theta}^s$ is also an unconstrained stationary point of m, i.e., $\nabla m(\boldsymbol{\theta}^s)=\mathbf{0}^T$. To second order, Eq. (7) reduces to (neglecting the ½ factor)

$$m(\boldsymbol{\theta}^s + \delta\boldsymbol{\theta}) \cong \delta\boldsymbol{\theta}^T \boldsymbol{H}^s \delta\boldsymbol{\theta} \tag{8}$$

where $\boldsymbol{H}^s$ is the Hessian matrix of m evaluated at the singular configuration. Expressing the gimbal angle variations as linear combinations of the Jacobian null space basis vectors, Eq. (8) reduces to

$$m(\boldsymbol{\theta}^s + \delta\boldsymbol{\theta}) \cong \boldsymbol{c}^T \boldsymbol{N}^T \boldsymbol{H}^s \boldsymbol{N} \boldsymbol{C} = \boldsymbol{c}^T \boldsymbol{W} \boldsymbol{c} \tag{9}$$

The quadratic form of Eq. (9) can now be used to test the possibility of escape. Because $m(\theta) \geq 0 \forall \theta$, $\boldsymbol{H}^s \geq 0$ and also $\boldsymbol{W} \geq 0$. A sufficient condition for escape by null motion is $\boldsymbol{H}^s > 0$; if sufficient condition for escape by null motion is $\boldsymbol{H}^s > 0$; if $\boldsymbol{W} > 0$, it is evident that escape is possible. When $\boldsymbol{W}$ is singular, Eq. (9) admits solutions $\boldsymbol{c}_w$ for which the quadratic form is zero. If these solutions coincide with the ones obtained from Eq. (4) (i.e., $\boldsymbol{c}_w = \boldsymbol{c}_s$), the test is inconclusive and other means must be used to characterize the nature of the stationary point (e.g., including higher-order terms). Such degenerate cases may appear if the stationary point is actually a closed curve in Θ. In this case, one might also numerically check whether $m(\boldsymbol{\theta}^s + \delta\boldsymbol{\theta})$ does not remain exactly zero along the variation in question.

In the practical application of this method, the computational burden of evaluating the Hessian matrix $\boldsymbol{H}^s$ can be reduced by applying the Binet-Cauchy[14] identity to express m as the sum of the Jacobian minors squared

$$m = \det(\boldsymbol{J}\boldsymbol{J}^T) = \sum_{i=1}^{p} M_i^2$$

where $p = n(n-1)(n-2)/3!$, $n \geq 3$, and M_i are the distinct Jacobian minors of order 3.

B. Examples of Internal Singularities

To illustrate the concepts introduced in this test, two examples of internal singularities are presented for a four-pyramid CMG system. The singular direction $\boldsymbol{s}$ for both cases is the spacecraft x axis. For simplicity, unit magnitude CMG momentum is assumed.

As an example of an elliptic internal singularity, consider the configuration $\boldsymbol{\theta}^s = [-90, 0, 90, 0]^T$ (in degrees) shown in Fig. 3. The singular direction $\boldsymbol{s}$ is the x axis. For this case

$$\boldsymbol{Q} = 2\begin{bmatrix} c\beta & c\beta^2 \\ c\beta^2 & c\beta^3 \end{bmatrix}$$

where $c\beta = \cos(\beta) > 0$, and β is the pyramid skew angle (54.73 deg). It is evident that null motion is impossible since $\boldsymbol{Q} > 0$.

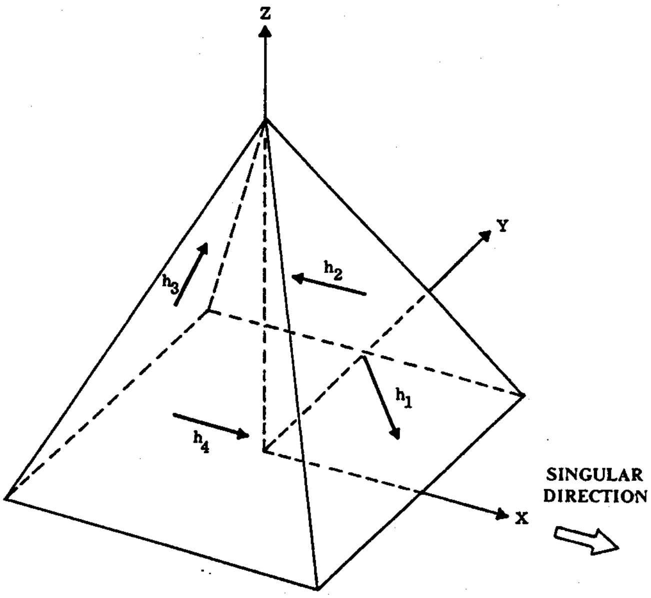

Fig. 3 Example of elliptic internal singularity.

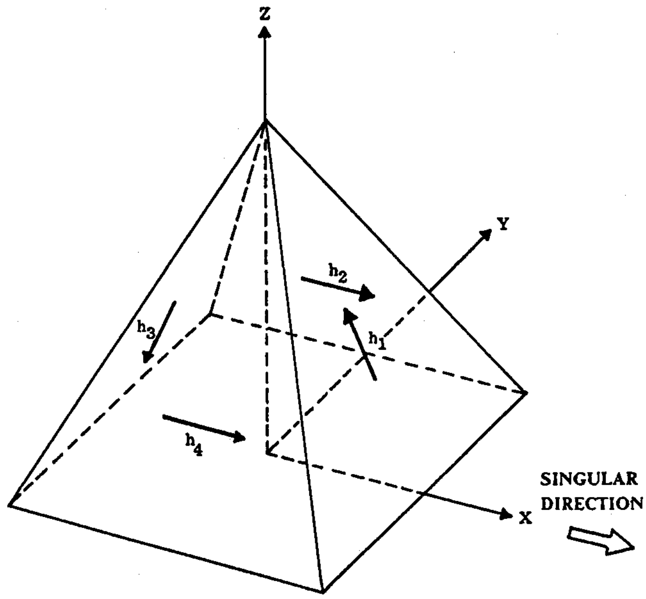

Fig. 4 Example of escapable hyperbolic internal singularity.

An escapable hyperbolic singularity is defined by $\boldsymbol{\theta}^s = [90, 180, -90, 0]$ (in degrees) shown in Fig. 4. For this case the quadratic polynomial of Eq. (6) is

$$(c_1 - 1.76c_2)(c_1 + 0.605c_2) = 0$$

Two sets of distinct null variations exist in this case and are given by

$$\delta\boldsymbol{\theta}_{a1} = c\begin{bmatrix} -0.605 \\ 1 \\ 1.76 \\ 1 \end{bmatrix} \qquad \delta\boldsymbol{\theta}_{a2} = c\begin{bmatrix} 1.76 \\ 1 \\ -0.605 \\ 1 \end{bmatrix}$$

For small values of the scaling constants c, it can be shown that Eq. (4) is satisfied. Evaluating the W matrix, we obtain

$$W = \begin{bmatrix} 4.741 & -2.737 \\ -2.737 & 8.536 \end{bmatrix}$$

In this case $W > 0$, and this singularity can be escaped by null motion.

VII. Conclusion

In this paper, the robotic manipulator was proposed as the mechanical analog to single gimbal control moment gyroscope (SGCMG) systems. It was shown that both systems possess similar behavior with regard to singular configurations, and that techniques from one area may be readily applicable to the other. An example of this was presented in the definition of families of gimbal angle solutions for any given momentum state. Not only is the analogy useful for generic analysis, it can also be exploited in the design of steering laws for redundant systems since singularity avoidance has been an active research area, and many steering strategies have been developed for kinematically redundant manipulators.

The singularity problem associated with SGCMG systems was examined in detail. A method was presented to test for the possibility of nontorque-producing gimbal motion at a singular configuration, as well as to determine the admissible motions in the case when this is possible. Sufficient conditions were derived for the case when the singular system can be reconfigured into a nonsingular state by these nontorque-producing motions. The concept of rigid-body null motion was introduced to define a class of degenerate null motion that is unable to affect the rank of the Jacobian and thus extricate the system from the singular state. In this case, criteria were derived by expanding the singularity measure as a function of null displacements whereby these motions provide for possibility of escape.

Acknowledgments

This paper was prepared by the Charles Stark Draper Laboratory, Inc., under Contract NAS9-17560 with NASA. The work was supported by the NASA Johnson Space Center. Publication of this report does not constitute approval by NASA of findings or conclusions contained herein. It is published for the exchange and stimulation of ideas. The helpful comments and suggestions of an anonymous reviewer were greatly appreciated.

References

[1]Crenshaw, J. W., "2-Speed, A Single Gimbal Control Moment Gyro Attitude Control System," *Proceedings of the AIAA Guidance and Control Conference,* AIAA, New York, 1973.

[2]Meffe, M., and Stocking, G., "Momentum Envelope Topology of Single-Gimbal CMG Arrays for Space Vehicle Control," *Proceedings of AAS Guidance and Control Conference*, Keystone, CO, Jan.–Feb. 1987, AAS Paper 87-002.

[3]Branets, V. N., "Development Experience of the Attitude Control System Using Single-Axis Control Moment Gyros for Long-Term Orbiting Space Stations," 38th Congress of the International Astronautical Federation, Brighton, UK, Oct. 1987, IAF Paper 87-04.

[4]Margulies, G., and Aubrun, N., "Geometric Theory of Single-Gimbal Control Moment Gyro Systems," *Journal of Astronautical Sciences,* Vol. 26, No. 2, 1978, pp. 159–191.

[5]Kurokawa, H., Yajima, S., and Usui, S., "A New Steering Law of a Single-Gimbal CMG System of Pyramid Configuration," *Proceedings of Xth IFAC Symposium on Automatic Control in Space*, Toulouse, France, June 1985, p. 249.

[6]Litvin, F. L., and Parenti, C. V., "Configurations of Robotic Manipulators and their Identification, and the Execution of Prescribed Trajectories. Part 1: Basic Concepts," *ASME Journal Mechanisms, Transmissions, and Automation in Design*, Vol. 107, No. 2, 1985, pp. 170–178.

[7]Borrel, P., and Liegeois, A., "A Study of Multiple Manipulator Inverse Kinematic Solutions With Applications to Trajectory Planning and Workspace Determination," *Proceedings of IEEE International Conference on Robotics and Automation*, Inst. of Electrical and Electronics Engineers, New York, 1986, pp. 9–14.

[8]Bedrossian, N. S., "Steering Law Design for Redundant Single Gimbal Control Moment Gyro Systems," M.S.M.E. Thesis, Massachusetts Inst. of Technology, Cambridge, MA, 1987.

[9]Cornink, D. E., "Singularity Avoidance Control Laws for Single Gimbal Control Moment Gyros," *Proceedings of the AIAA Guidance and Control Conference*, AIAA, New York, Aug. 1979, pp. 20–23.

[10]Spivak, M., *Calculus On Manifolds,* W. A. Benjamin, Inc., New York, 1965.

[11]Bauer, S. R., "Difficulties Encountered in Steering Single Gimbal CMGs," Charles Stark Draper Lab., Cambridge, MA, Space Guidance & Navigation Memo 10E-87-09, June 1987.

[12]Hogan, N., "Impedance Control: An Approach to Manipulation: Part II—Implementation," *ASME Journal of Dynamic Systems, Measurement, and Control*, Vol. 107, March 1985, pp. 8–16.

[13]Bedrossian, N. S., "Singular Configurations of Kinematically Redundant Manipulators," *Proceedings of the IEEE International Conference on Robotics and Automation,* Inst. of Electrical and Electronics Engineers, New York, 1990, pp. 818–823.

[14]Gantmacher, F. R., *Theory Of Matrices,* Chelsea, New York, 1959.